J Nanostruct 11(3): 618-627, Summer 2021

RESEARCH PAPER

The Nearly Perfect Optical Filter Composed of [SiO_2/ZrO_2] Stacks using One-Dimensional Photonic Crystals

*Saman Mahmoodi, Mehrdad Moradi *, and Farideh Sadat Saeidi*

Institute of Nanoscience and Nanotechnology, University of Kashan, Kashan 87317, Iran

ARTICLE INFO

Article History:
Received 05 April 2021
Accepted 24 June 2021
Published 01 July 2021

Keywords:
Electric field distribution
Laser safety
Photonic crystal
Thin film
Transfer matrix method

ABSTRACT

In this paper, a one-dimensional photonic crystal (PhC) composed of [SiO_2/ZrO_2] stacks is designed to act as an optical filter. These types of filters have been extensively used in safety glasses working in the wavelength of 355 nm. Here, theoretical calculations are carried out in MATLAB software based on the transfer matrix method (TMM). Simulations showed that the structure of Quartz/[SiO_2/ZrO_2]^{20} can block the wavelength of 355 nm, reducing the transmittance ratio to 1.29×10^{-5}%. By forming 16 stacks, the optical density (OD) reaches 5, completely protecting the user's eyes from laser beams with incident angles ranging from 0 to 22 degrees. For higher incident angles up to 38 degrees, 20 stacks of [SiO_2/ZrO_2] are needed to reach OD = 5. The visible light can pass through this filter about 70%, being sufficient for the user's vision. Finally, the distribution of the electric field is simulated to confirm the performance of the resulting structures.

How to cite this article
Mahmoodi S, Moradi M, and Saeidi F. The Nearly Perfect Optical Filter Composed of [SiO_2/ZrO_2] Stacks using One-Dimensional Photonic Crystals. J Nanostruct, 2021; 11(3):618-627. DOI: 110.22052/JNS.2021.03.019

INTRODUCTION

Photonic crystals (PhCs) are multilayer structures that have repeated stacks of the dielectric layers with different refractive indices (low and high). The period in the refractive indices led to a blocking band which is barricaded photon emission in the structure. In accordance with the structural periodicity of photonic crystals, they can be classified into three different classifications: one-dimensional (1-D), two-dimensional (2-D), and three-dimensional (3-D). Consequently, photonic crystals have drawn global attention for their use in various applications such as Bragg mirrors, reflectors, optical filters, and laser eye protection filters [1-7]. Laser users must adhere to specific safety principles due to the high focusing and high intensity of light. Because of a high concentration of visible and near-infrared radiation on the retina, it is the most vulnerable to laser radiation. Retinal laser injuries are characterized by a sudden loss of vision, often followed by marked improvement over a few weeks, and occasionally severe late complications. In this case, medical and surgical treatments are limited. Therefore, prevention and eye protection are very essential [8-12]. In this situation, not only a direct beam of the laser is hazardous to the health of the user, but also a reflected beam [13,14] and dispersed beam can be dangerous when scattered from the diffuser targets. In addition, high-power lasers with low wavelength (lasers class 3R and above) place on a higher risk level [15,16]. Because this type of lasers have a lot of energy and according to the high centralization, their peril is far higher, therefore, observance of safety principle is more imperative during work with them. Different types of eye-protective devices have been designed for different circumstances. While for average optical

* *Corresponding Author Email: m.moradi@kashanu.ac.ir*

power, optical glasses with a plastic filter are used, in which these kinds of glasses are made up of polycarbonate or a layer of absorbent or reflective [17], for higher power, the actual glass is used. Glass has better resisted against the laser beam and also against scratches; however, it is very weak against mechanical shocks. Another type of glasses can be made of multilayer dielectric [18], nanogratings [19] or 1D-PhCs [7] to act as the Bragg mirror against direct wavelengths. Not only can these mirrors act as a full mirror, but also they are able to pass a particular wavelength from the crystal by creating a defect in their structure. The optical properties of the structure and the characteristics of the filter can be manipulated and controlled according to its application by monitoring the type of layers, their thicknesses, the number of repetitions, and defects in the structure [20, 21].

Regarding the importance of laser safety, in this paper, a photonic blocker of Quartz/$[SiO_2/ZrO_2]^n$ is designed to use in safety goggles for 355 nm laser. Here, we use quartz instead of BK7 because the BK7 has a large absorption in the ultraviolet region. There is no refractive index measured for BK7 in the ultraviolet region also the loss of UV-light intensity in it would add up to the optical blocking of the PhC. Therefore quartz was selected as the base of the safety goggles, also zirconium dioxide (ZrO_2) and silicon dioxide (SiO_2) are used as high and low refractive indexes, respectively. SiO_2 is a very well-known dielectric that has been used in PhCs widely [22-24]. In our based calculations several materials have been chosen to match with SiO_2 in the PhC which led to picking the ZrO_2 as the high refractive indexes in the structure [25]. It's worth mentioning that the absorption coefficient of these dielectric materials is near zero for the UV-Vis spectra which are perfect for our purpose [25, 26]. Different PhCs have been designed with different combinations and details containing SiO_2 or even SiO_2/ZrO_2 [23-24,27]. What makes this paper special is that we focus on filtering certain wavelength with a goggle and reducing the laser transmittance enough to make it safe for a human's eye to work with 355 nm lasers that are used for laser medical treatments, microscopy, flow cytometry, Raman spectroscopy, and micro-electronics manufacturing

THEORETICAL PRINCIPLES

Periodic structures and PhCs are discussed using Maxwell's equations [28, 29]. Generally, the beam of light is considered an electromagnetic plane wave $\vec{E}(r) = E_0 e^{i(\vec{k}\cdot\vec{r}-\omega t)}$ (Fig. 1).

According to the boundary condition for electric fields and magnetic fields, all tangential components are continuous:

$$\mathrm{E}_1^{\parallel} - \mathrm{E}_2^{\parallel} = 0, \frac{\mathrm{B}_1^{\parallel}}{\mu_1} - \frac{\mathrm{B}_2^{\parallel}}{\mu_2} = 0 \quad (1)$$

$$\mathrm{E_i} + \mathrm{E_{1r}} = \mathrm{E_t} + \mathrm{E_{2r}} \quad (2)$$

$$\mathrm{H_i} + \mathrm{H_{1r}} = \mathrm{H_t} + \mathrm{H_{2r}}, \mathrm{n_0\ E_i cos\theta_i} - \mathrm{n_0\ E_{1r} cos\theta_i} = \mathrm{n_1\ E_{1t} cos\theta_t} - \mathrm{n_1\ E_{2r} cos\theta_t} \quad (3)$$

where E_i and H_i are the incident beams, E_{1r} and H_{1r} are the reflected beams from the LHS of the z=0, and are the transmitted beams, and E_{2r} and H_{2r} are the reflected beams from the RHS of interface z=0. Then can rewrite the above equations in a matrix form:

$$\begin{pmatrix} 1 & 1 \\ n_0 cos\theta_i & -n_0 cos\theta_i \end{pmatrix} \begin{pmatrix} E_i \\ E_{1r} \end{pmatrix} = \begin{pmatrix} 1 & 1 \\ n_1\, cos\theta_t & -n_1 cos\theta_t \end{pmatrix} \begin{pmatrix} E_t \\ E_{2r} \end{pmatrix} = A_0 \begin{pmatrix} E_i \\ E_{1r} \end{pmatrix} = DAA_1 \begin{pmatrix} E_t \\ E_{2r} \end{pmatrix} \quad (4)$$

$$A_1^{-1} A_0 \begin{pmatrix} E_i \\ E_{1r} \end{pmatrix} = \begin{pmatrix} E_t \\ E_{2r} \end{pmatrix} \quad (5)$$

where A is called the dynamical matrix. Also, for the emission of light in a thin film, the propagation matrix is defined as:

$$D_i = \begin{bmatrix} e^{-ik_i L_i} & 0 \\ 0 & e^{+ik_i L_i} \end{bmatrix} \quad (6)$$

the k_i is the wavenumber of the i^{th} layer and L is the distance that light traveled inside the thin film. In periodic structures with a large number of layers, the above equations are expressed as follows:

$$\begin{bmatrix} E_i \\ E_{1r} \end{bmatrix} = A_0^{-1} [A_1 D_1 A_1^{-1} A_2 D_2 A_2^{-1}]^N A_s \begin{bmatrix} E_t \\ E_{2r} \end{bmatrix} \quad (7)$$

$$\begin{bmatrix} E_i \\ E_{1r} \end{bmatrix} = \begin{bmatrix} \mathrm{M_{11}} & \mathrm{M_{12}} \\ \mathrm{M_{21}} & \mathrm{M_{22}} \end{bmatrix} \begin{bmatrix} E_t \\ E_{2r} \end{bmatrix} \quad (8)$$

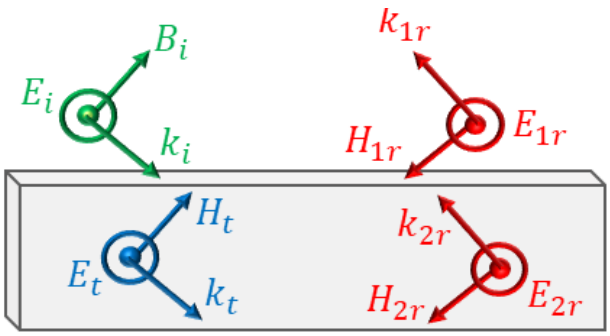

Fig. 1. Electromagnetic plane wave at the interface of two layers.

where 0 and S denote air and substrate, respectively. The matrix M is the total matrix of the structure and by using this matrix, the Fresnel coefficients and reflectivity and transmission of structure can be calculated subsequently, as follows [30,31]:

$$r=M_{21}/M_{11} \quad (9)$$

$$t=1/M_{11} \quad (10)$$

where $M_{(m,n)}$ is an element in the m^{th} row and n^{th} column, of M matrix. The total electric field expression of the TE and TM polarizations as follows:

$$\begin{bmatrix}1\\ r\end{bmatrix} = M \begin{bmatrix}E_R\\ E_L\end{bmatrix} \quad (11)$$

where is the forward propagating electric field components, and E_L is the backward propagating electric field components of the whole structure:

$$E = E_R + E_L \quad (12)$$

$$I = |E|^2 . \quad (13)$$

Finally, the optical density (OD) defined as [32]:

$$OD = \log_{10}\left(\frac{I_i}{I_t}\right) \quad (14)$$

where I_i is the incident light intensity and I_t is transmitted light intensity.

CALCULATIONS AND SIMULATION

For simulations of PhC, quartz plays the role of the substrate also zirconium dioxide (ZrO_2) and silicon dioxide (SiO_2) are selected as thin films with high and low refractive indices, respectively. In calculations, the refractive indices of quartz [33], silicon dioxide [26] and zirconium dioxide [25] were extracted from references and illustrated in Fig. 2. It's worthy to mention that all three of Quartz, SiO_2, and ZrO_2 are dielectrics with almost zero extinction of light which means their imaginary parts of the refractive index are negligible in the UV-visible spectrum. Blocking PhC has been designed for 355-nm UV laser, regarding this goal some parameters such as working wavelength (WW), layer's thickness and the number of stacks have to be optimized. It's well known layers thickness in PhCs are calculated using $L=\lambda_w/4n$ equation where λ_w is WW.

To scrutiny of WW, the structures with WWs of 250, 300, 355, 400 and 450 nm were simulated. The intensity of transmitted light from the structure with 10 stacks of [SiO_2/ZrO_2] was calculated and results were shown in Fig. 3. In results for each WW, there is a blocking band about 100 nm width that the related WW almost place in the middle of the blocking band. Besides, in the other regions of the spectrum, the transmitted light is not diminish appreciably. Therefore, the structure acts as a perfect filter in the desired range and it passes other wavelengths. Consequently, regarding the paper's target, the WW of 355 nm was selected.

After the determination of the WW, the related thicknesses of 59 and 38 nm were obtained using $L=\lambda_w/4n$ equation for silicon dioxide and zirconium dioxide, respectively. Now, with more calculations, it is possible to obtain the optimum number of stacks to obtain optimal conditions and the desirable blocking rate. In this way, the intensity of light transmission of the structure was calculated for n = 5, 10, 15 and 20 (where n is the repetitions of [SiO_2/ZrO_2] stacks) and results were

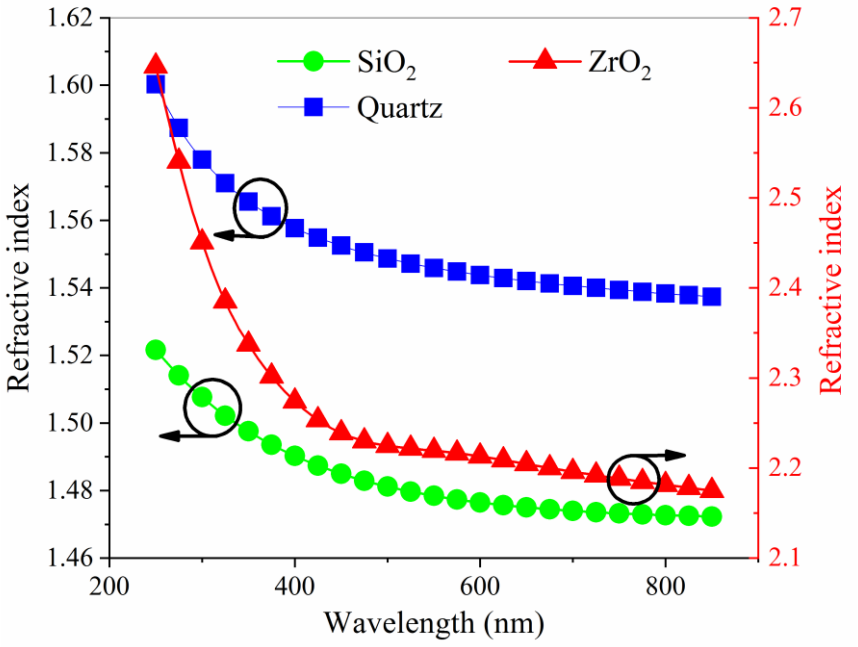

Fig. 2. Refractive index of Quartz [33], SiO_2 [26] and ZrO_2 [25] versus wavelength, imaginary parts of refractive index are negligible.

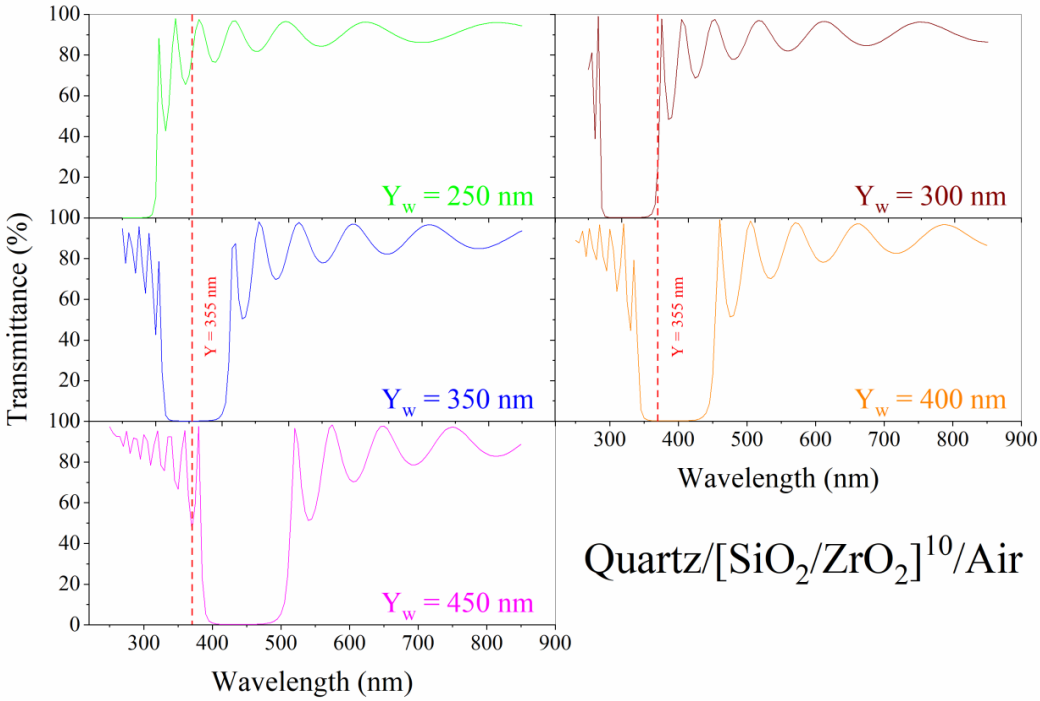

Fig. 3. The transmittance spectrum of Quartz/$[SiO_2/ZrO_2]^{10}$ structure for the WWs of 250, 300, 355, 400 and 450 nm.

demonstrated in Fig. 4. One can see the blocking effect does not satisfy completely in n= 5 but by increasing the value of n, up to 10, the blocking effect has improved in the wavelength region of 335-375 nm, but still, this effect is not optimum and merely some part of the light is transmitted (see Fig. 4). Ultimately, in the structure with n=15, the filter effect of PhC has an acceptable condition

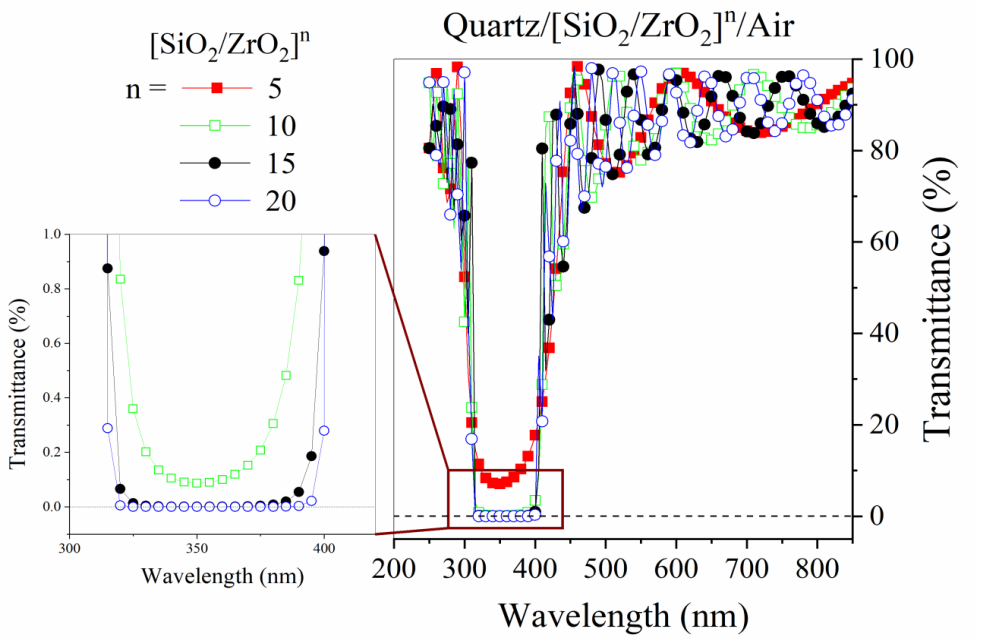

Fig. 4. The transmittance of Quartz/$[SiO_2/ZrO_2]^n$ structure with n = 5, 10, 15, and 20. Inset image shows the blocking band area in more detail.

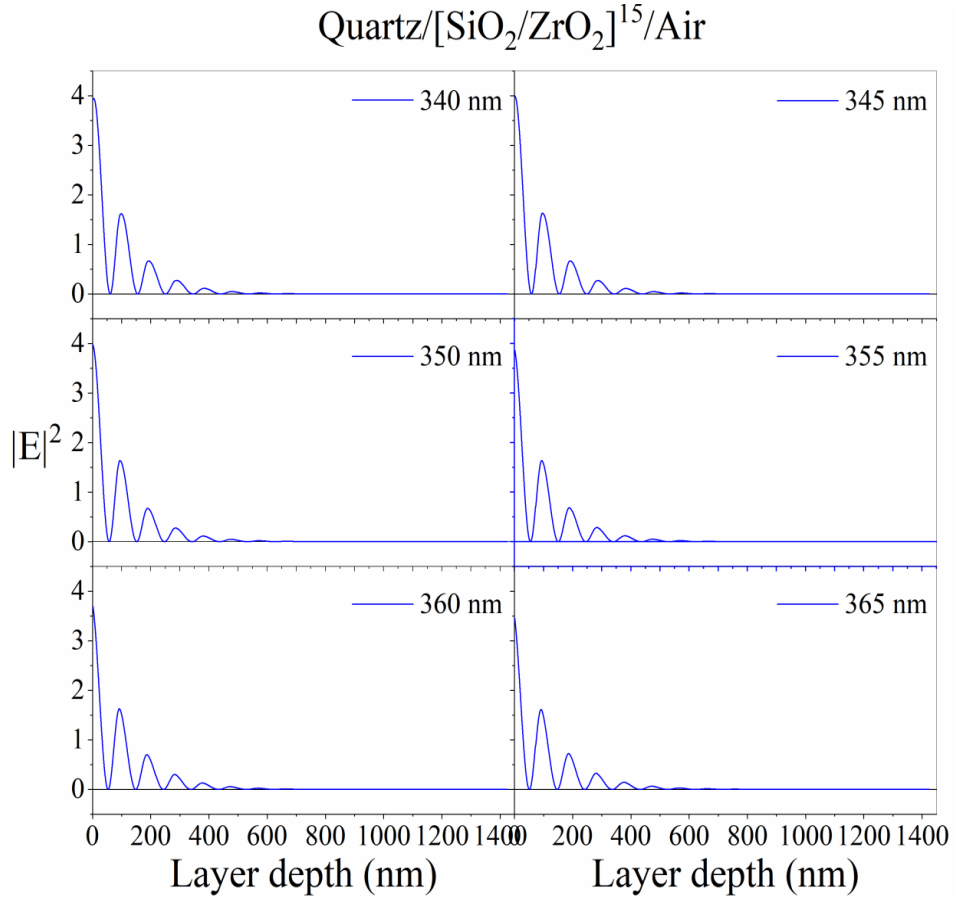

Fig. 5. The distribution function of electric field intensity in the PhC filter with Quartz/$[SiO_2/ZrO_2]^{15}$ structure for wavelengths of 340, 345, 350, 355, 360 and 365 nm.

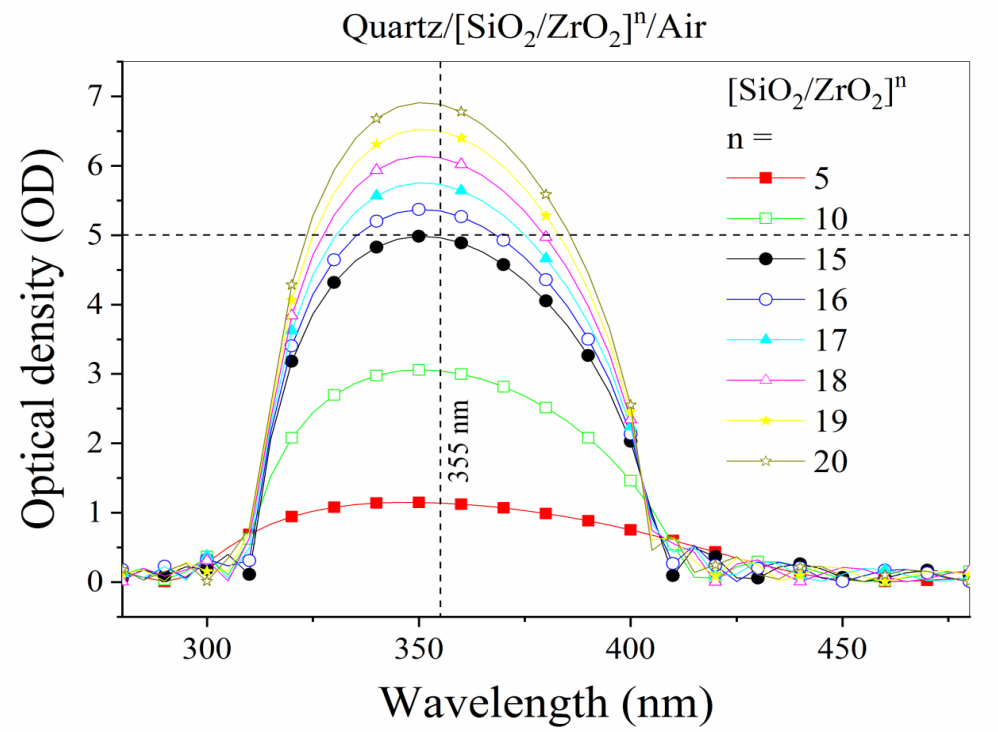

Fig. 6. Optical density of structure versus wavelength for different numbers of 5, 10, 15, 16, 17, 18, 19 and 20 [SiO_2/ZrO_2] stacks.

and with increasing the n value up to 20, the blocking quality reach perfection. In this structure, the light transmittance reduces to less than 1.29×10^{-5}% at the wavelength of 355 nm which is very desirable and satisfactory.

Studying the distribution function of the electric field intensity in the structure is very useful and can provide a better understanding of structure performance [28,34,35]. In this regard, to ensure the performance of the filter, the transmission distribution function was plotted for wavelengths near 355 nm i.e. 340, 345, 350, 360 and 365 nm and was shown in Fig. 5. In this figure, X-axis presents the depth of the structure starting from the air side. Here the distribution of the field intensity in 15 stacks [SiO_2/ZrO_2] has been calculated using the Matlab code. This code works in a for loop that starts with calculation of the distribution of the field intensity in depth of 1 nm which is SiO_2 and goes forward till it gets to the SiO_2/ZrO_2 boundary, there for code calculates the distribution of the field intensity in one layer of SiO_2 and 1 nm layer of ZrO_2 and so on. According to Fig. 5, the filter proceeds of a PhC were again confirmed for the wavelength of 355 nm and nearby wavelengths around it. The distribution of the field intensity curve demonstrated that how the electric field of a laser beam had merely aspired to zero at the depth of layer and nearby the quartz substrate. Consequently, the beam was completely blocked and the high energy waves did not reach the user's eyes, thus, safety was guaranteed.

As we know the laser beams with different wavelengths have different effects on the human ocular system. Lasers with ultraviolet wavelength potentially are hazardous for the cornea since these wavelength ranges will focus on the cornea and will cause damage. The cornea is the part of the ocular system that absorbs ultraviolet wavelength, therefore this type of lasers are harmful to the cornea. Based on the type of lasers, the damage mechanisms caused by them are different. Continuous wavelength (CW) lasers cause burning (thermal process) and photochemical degeneration (UV effect) [36]. Pulsed lasers cause thermal and photochemical processes also blast damage along with damage that come from shock and acoustic waves of these pulsed lasers. The laser caused injuries are determined by multiple laser-related and eye-related factors such as laser wavelength, exposure time, laser power, direct contact or indirect exposure and etc. Lots

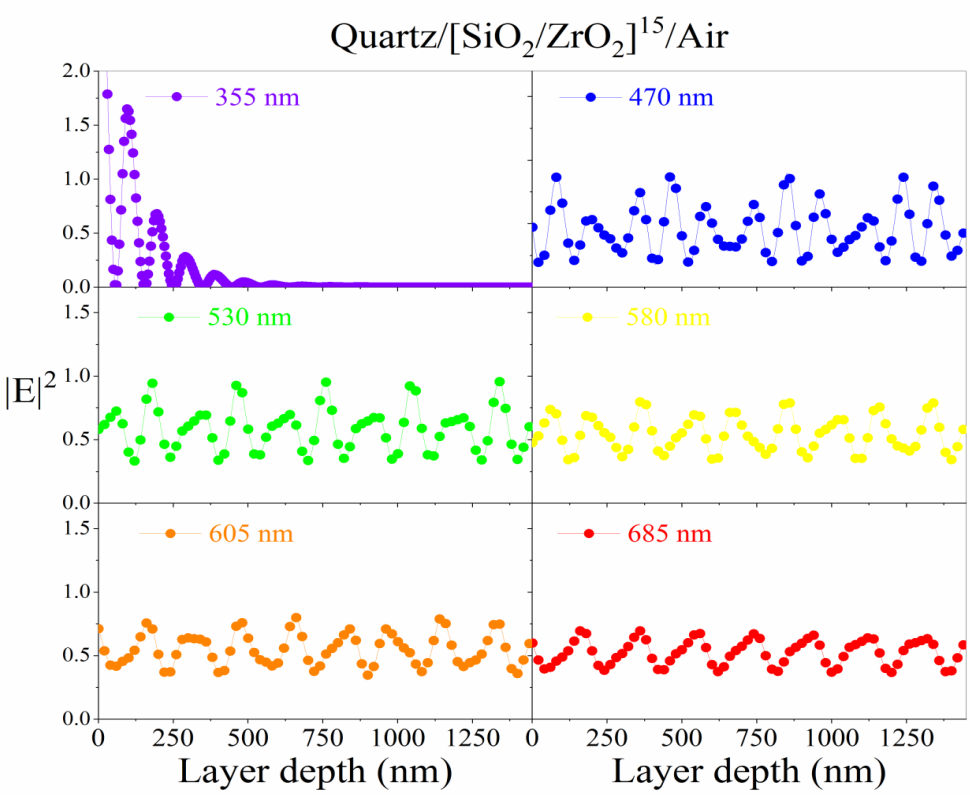

Fig. 7. The distribution function of electric field intensity in the PhC blocking filter with Quartz/[SiO_2/ZrO_2]^{15} structure for wavelengths of 355, 470, 530, 580, 605 and 685 nm (UV and visible light ranges).

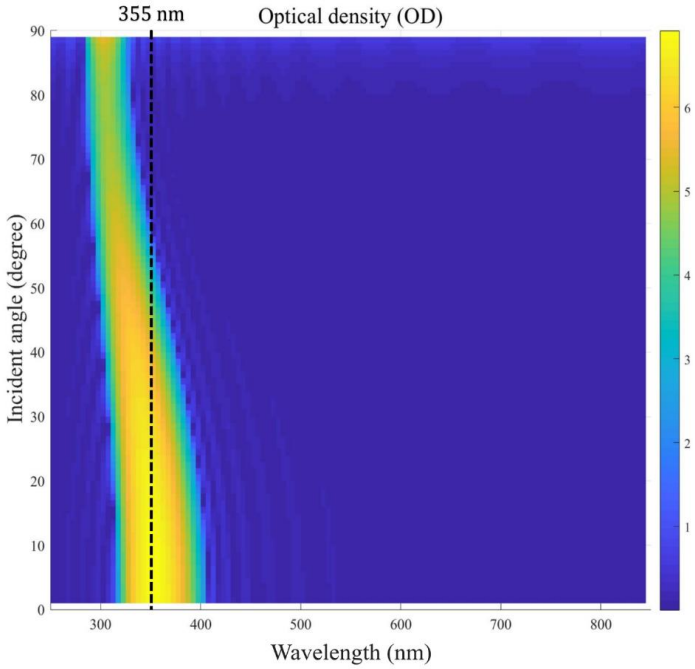

Fig. 8. Optical density for incident angles of 0 to 90 degrees versus wavelength calculated for Quartz/[SiO_2/ZrO_2]^{15}.

Table 1. The electric field intensity in the ending point of the blocking filter ($|E_{end}|^2$) for different wavelengths of 355, 470, 530, 580, 605 and 685 nm (UV and visible light ranges).

Wavelength	355 nm	470 nm	530 nm	580 nm	605 nm	685 nm
$\|E_{end}\|^2$	7.28×10^{-6}	0.46	0.64	0.61	0.63	0.60

of studies took place on ocular system and skin laser damage threshold.One of the standards for laser safety filters is optical density (OD) which is defined as equation (14). The minimum of OD is about 5 required to eliminate the risk of lasers [32]. Considering previous discussion OD of the designed PhC filter for WW of the 355 nm and the different numbers of 5, 10, 15, 16, 17, 18, 19 and 20 $[SiO_2/ZrO_2]$ stacks have been calculated and presented in Fig. 6. The intersecting lines (dash lines) of OD=5 and λ=355 nm show that 5 and 10 stacks of $[SiO_2/ZrO_2]$ won't offer safety, but with increasing the number of stacks up to 15, the OD curve almost reaches 5, which promises safety for its user. By increasing the number of stacks higher than 15, (n= 16-20), the OD curves go higher and cover a wide range of wavelengths with desirable OD.

For a safety goggle, the whole subject doesn't necessarily evolve just around blocking the light, we need to avoid blocking visible range and not disturbing user's vision. In this regard, six wavelengths in the visible spectra were chosen and the distribution function of the electric field of related wavelengths throw depth of structure with 15 stacks were calculated and illustrated in Fig. 7. Field distribution results prove and discuss the results of Fig. 5 in another way. The electric field intensity at the end of the structure that entitled $|E_{end}|^2$ is listed in Table 1. One can see that the designed filter does nothing much to the visible spectra and besides blocking ultraviolet region and safety, won't interrupt with the user's vision.

All the pre simulations and discussions before were for the ideal situation where light incidents on the filter surface perpendicularly. The extra simulations and calculations were carried out for gaining more realistic insight about the designed structure capabilities and weaknesses. Fig. 8 presents the optical density of structure with 15 stacks of $[SiO_2/ZrO_2]$ in wavelengths of 250 to 800 nm versus incident angles in ranges 0 to 90 degrees. Fig. 8 shows with increasing the incident angle to about 40 degrees, the OD's peak width which is related and homologous to blocking band doesn't change a lot. For incident angles larger than 40 degrees, the OD peak gets narrow and shifts to lower wavelengths which is not desirable.

The main wavelength in this paper is 355 nm, therefore, OD for 355 nm on the structure with

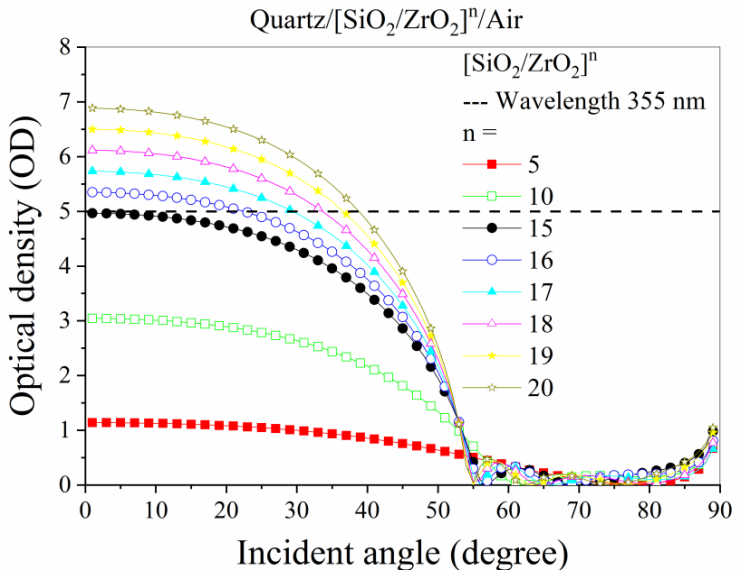

Fig. 9. The optical density of structure for wavelength of 355 nm versus incident angles of 0 to 90 degrees for different numbers of 5, 10, 15, 16, 17, 18, 19 and 20 $[SiO_2/ZrO_2]$ stacks.

Table 2. Safe incident angle region for different numbers of [SiO_2/ZrO_2] stacks carried out in Fig. 10 (NS means not safe).

Number of stacks	5	10	15	16	17	18	19	20
Safe incident angle ranges (degree)	NS	NS	NS	0 to 22	0 to 29	0 to 33	0 to 36	0 to 38

5, 10, 15, 16, 17, 18, 19 and 20 stacks of [SiO_2/ZrO_2] versus incident angles of 0 to 90 degrees are calculated and shown in Fig. 9. Also, table 2 presents the safe incident angle range for 5, 10, 15, 16, 17, 18, 19 and 20 stacks of [SiO_2/ZrO_2]. The results show that n = 1, 5, 10 and 15 stacks can't be trusted and don't offer any safety but for 16 stacks, users can make sure direct stroked laser beam with incident angles ranging from 0 to 22 degrees won't cause any damage. By increasing the number of stacks up to 20, the user is safe against the direct strike ranging from 0 to 38 degrees.

CONCLUSION

In this paper, an optical filter consisting of the PhC with repetitions of [SiO_2/ZrO_2] stacks was designed and investigated. Here, thicknesses of the silicon dioxide and zirconium dioxide were selected to be 59 and 38 nm, respectively. Various parameters of the blocking filter were studied and calculated for the wavelength of 355 nm of high-energy lasers, thereby designing a high-efficiency blocking filter with an OD of at least 5. Simulations showed that the structure of Quartz/[SiO_2/ZrO_2]^{20} can block the wavelength of 355 nm, reducing the transmittance to 1.29×10^{-5} %. By having 16 stacks and higher, the optical density reached 5, completely protecting the user's eyes from laser beams with incident angles ranging from 0 to 22 degrees. For incident angles up to 38 degrees, 20 stacks of [SiO_2/ZrO_2] guaranteed no damage to the eyes of the operator. This filter transmits at least 70% of the visible light, being enough for the user's vision. Finally, the distribution of the electric field was also used to confirm the performance of the structures.

CONFLICT OF INTEREST

The authors declare that there is no conflict of interests regarding the publication of this manuscript.

REFERENCES

1. Moradi M, Alisafaee H, Ghanaatshoar M. The Kerr effect enhancement in non-quarter-wave lossy magnetophotonic crystals. Physica B. 2010;405(21):4488-4491.
2. Seifouri M, Fallahi V, Olyaee S. Ultra-high-Q optical filter based on photonic crystal ring resonator. Photonic Netw Commun. 2018 2018/04/01;35(2):225-230.
3. Sahel S, Amri R, Bouaziz L, et al. Optical filters using Cantor quasi-periodic one dimensional photonic crystal based on Si/SiO_2. Superlattices Microstruct. 2016;97:429-438.
4. Ghanaatshoar M, Zamani M, Alisafaee H. Compact 1-D magnetophotonic crystals with simultaneous large magnetooptical Kerr rotation and high reflectance. Opt Commun. 2011;284(14):3635-3638.
5. Zamani M, Ghanaatshoar M. High performance reflection-type 1D magnetophotonic crystals with flat-top responses. Photonics Nanostructures: Fundam Appl. 2013;11(3):234-240.
6. Calvo M.E, Sobrado O.S, Lozano G, Miguez H. Molding with nanoparticle-based one-dimensional photonic crystals: a route to flexible and transferable Bragg mirrors of high dielectric contrast. J. Mater. Chem. 2009; 19:3144–3148.
7. Chen M, Li C, Xu M, et al. Eye-protection glasses against YAG laser injury based on the band gap reflection of one-dimensional photonic crystal. Opt Laser Technol. 2007;39(1):214-218.
8. Barkana Y, Belkin M. Laser eye injuries. Surv Ophthalmol. 2000;44(6):459-478.
9. Birtel J, Harmening WM, Krohne TU, et al. Retinal injury following laser pointer exposure: a systematic review and case series. Dtsch Arztebl Int. 2017;114(49):831.
10. Xu K, Chin EK, Quiram PA, et al. Retinal injury secondary to laser pointers in pediatric patients. Pediatrics. 2016;138(4):e20161188.
11. Lund DJ, editor Time dependence of laser-induced retinal thermal injury. International Laser Safety Conference; 2019: Laser Institute of America.
12. Yiu G. Retinal Laser Injury. Elsevier; 2020. (Handbook of Pediatric Retinal OCT and the Eye-Brain Connection).
13. Thanos S, Böhm MR, zu Hörste MM, et al. Retinal damage induced by mirror-reflected light from a laser pointer. J BMJ case reports. 2015;2015:bcr2015210311.
14. Sourial MW, Knudsen BE. Ho: YAG Laser Lithotripsy. Ureteroscopy: Springer; 2020. p. 101-112.
15. Smalley PJ. Laser safety: Risks, hazards, and control measures. Laser Ther. 2011;20(2):95-106.
16. KingCLSO JJ, editor Beyond class 4, laser safety controls for very high-power lasers. International Laser Safety Conference; 2019: Laser Institute of America.
17. Actis-Datta SY, inventor; Bacou-Dalloz Eye & Face Protection Inc, assignee. Safety glasses with flexible frame and interchangeable dual-lenses. US2005.
18. Ahmed K, Khan A, Rauf A, et al., editors. Design and development of laser eye protection filter. J. Phys. Conf.; 2013: IOP Publishing.
19. Andreeva Y, Koval V, Sergeev M, et al. Picosecond laser writing of Ag–SiO_2 nanocomposite nanogratings for optical filtering. Opt Laser Eng. 2020 2020/01/01/;124:105840.
20. O'Sullivan F, Celanovic I, Jovanovic N, et al. Optical characteristics of one-dimensional Si⁄SiO_2 photonic crystals for thermophotovoltaic applications. J Appl Phys. 2005;97(3):033529.
21. Xiao X, Wenjun W, Shuhong L, et al. Investigation of defect

modes with Al_2O_3 and TiO_2 in one-dimensional photonic crystals. Optik. 2016;127(1):135-138.
22. Dalmis R, Ak Azem NF, Birlik I, et al. SiO_2/TiO_2 one-dimensional photonic crystals doped with Sm and Ce rare-earth elements for enhanced structural colors. Applied Surface Science. 2019 2019/05/01/;475:94-101.
23. Zhang W, Lv D. Preparation and characterization of Ge/TiO_2//Si/SiO_2 one-dimensional heterostructure photonic crystal with infrared spectrally selective low emissivity. Opt Mater. 2019 2019/10/01/;96:109333.
24. Merbati A, Bensliman A, Issani H, et al. Design and optimization of one-dimensional TiO_2/SiO_2 photonic crystal for thermophotovoltaic filter. J Ovonic Res. 2020;16(5):261-265.
25. filmetrics, website, https://www.filmetrics.com/refractive-index-database/ZrO_2/Zirconium-Dioxide. https://www.filmetrics.com/refractive-index-database/ZrO2/Zirconium-Dioxide.
26. Gao L, Lemarchand F, Lequime M. Refractive index determination of SiO_2 layer in the UV/Vis/NIR range: spectrophotometric reverse engineering on single and bi-layer designs. J Eur Opt Soc-Rapid. 2013;8:13010.
27. M. Bouras, N. Dermeche, A. Kahlouche and A. HOCINI, Modeling of photonic band gap in 1D magneto-photonic crystals made by SiO_2/ZrO_2 or SiO_2/TiO_2 doped with magnetic nanoparticles, 2020 International Conference on Electrical Engineering (ICEE), 2020, 1-4, doi: 10.1109/ICEE49691.2020.9249944.
28. Ayareh Z, Mahmoodi S, Moradi M. Magneto-plasmonic biosensing platform for detection of glucose concentration. Optik. 2019;178:765-773.
29. Lalanne P. Physics, Theory, and Applications of Periodic Structures in Optics. Bellingham, Wash., USA; 2001.
30. Mahmoodi S, Moradi M, Mohseni S. Optimization of magneto-optical Kerr effect in Cu/Fe/Cu nano-structure. J Supercond Nov Magn. 2016;29(6):1517-1523.
31. F.S. Saeidi, M. Moradi, A new route to designing a one-dimensional multiperiodic photonic crystal with adjustable photonic band gap and enhanced electric field localization, Optics Communications, 2021;493:126999.
32. Meredith WJ, Massey JB. Chapter XVI - The properties of the X-ray film. In: Meredith WJ, Massey JB, editors. Fundamental Physics of Radiology (Third Edition): Butterworth-Heinemann; 1977; 175-190.
33. Ghosh G. Dispersion-equation coefficients for the refractive index and birefringence of calcite and quartz crystals. Opt Commun. 1999;163(1-3):95-102.
34. Ayareh Z, Moradi M, Mahmoodi S. Tuning the effective parameters in (Ta/Cu/[Ni/Co] x/Ta) multilayers with perpendicular magnetic anisotropy. Physica C. 2018;m549:30-32.
35. Mahmoodi S, Moradi M. Carbon Nanotube Assisted Enhancement of the Magneto-Optical Kerr Signal in Nickel Thin Films. J Electron Mater. 2018;47(12):7069-7074.
36. A. Douplik, G. Saiko, I. Schelkanova, V.V. Tuchin, The response of tissue to laser light, Lasers for Medical Applications, Woodhead Publishing, 2013; 47-109.